Published in final edited form as:

Lab Chip. 2019 September 10; 19(18): 3094–3103. doi:10.1039/c9lc00399a.

A microscale, full-thickness, human skin on a chip assay simulating neutrophil responses to skin infection and antibiotic treatment

Jae Jung Kim[1,2], **Felix Ellett**[2], **Carina N. Thomas**[1], **Fatemeh Jalali**[2], **R. Rox Anderson**[1], **Daniel Irimia**[2,*], **Adam B. Raff**[1,*]

[1]Wellman Center for Photomedicine, Department of Dermatology, Massachusetts General Hospital, Harvard Medical School, Boston, Massachusetts, USA.

[2]BioMEMS Resource Center, Department of Surgery, Massachusetts General Hospital, Harvard Medical School, and Shriners Hospital for Children, Boston, Massachusetts, USA.

Abstract

Human skin models are essential for understanding dermatological diseases and testing new treatment strategies. The use of skin biopsies *ex vivo* is the most accurate model. However, their use is expensive and exposes the donor to pain and scarring. While bioengineered skin samples provide a cheaper alternative, they have limitations due to their simple structure and functionality compared to human skin. Here, we present a skin-on-a-chip device designed to study neutrophil responses to *Staphylococcus aureus* skin infections. We integrate human skin microcolumns, which have a cross-section that is ~100 times smaller than traditional skin biopsies, are full-thickness, and are collected using minimally invasive skin sampling techniques. We use human neutrophils directly from one drop of blood, without the need for blood separation. Using the skin-on-a-chip device with skin and blood samples from healthy donors, we show that the neutrophil responses correlate with the bacteria-load in the skin. A pre-incubation step increases the number of migrating neutrophils in response to a low concentration of bacteria. Antibiotic treatment of *S. aureus*-infected skin samples reduces the number of neutrophils migrating towards the skin. Overall, we validate a skin on a chip model that enables the study of neutrophil migration to the skin in the presence of microbes and following the administration of antibiotics, two situations relevant to clinical cases of human skin and soft tissue infections.

Introduction

Skin and soft tissue infections (SSTIs) are some of the most common reasons to seek medical care in the United States (US).[1] Cellulitis accounts for the majority of SSTIs and is most often caused by *Staphylococcus aureus* and *Streptococcus pyogenes*.[2] In the US, 14.5 million cellulitis cases annually account for $3.7 billion in ambulatory care costs.[1, 3] Unfortunately, one-third of these patients are misdiagnosed due to the many clinical mimics

* dirimia@mgh.harvard.edu; araff@bidmc.harvard.edu.

Conflicts of interest

There are no conflicts to declare.

of cellulitis, known collectively as pseudo-cellulitis.[4] Incomplete understanding of cellulitis biology leads to ineffective diagnostic strategies,[5–7] and overuse of broad-spectrum antibiotics.[4] At present, the majority of cellulitis cases are diagnosed based on history and physical exam findings. Unfortunately, the typical cellulitis exam findings of skin redness, warmth, pain, and swelling are common to many non-infectious, inflammatory skin conditions, leading to frequent misdiagnosis.[5–7] Common infection biomarkers, including white blood cell count, erythrocyte sedimentation rate, C-reactive protein, and procalcitonin, are neither sensitive nor specific for cellulitis.[8–11] Bacterial cultures from patients with cellulitis are negative more than 80% of the time.[12, 13] Even when positive, the concentration of bacteria is low.[10, 14] Skin histology from cellulitis demonstrates dermal edema, lymphatic dilation, and diffuse, heavy neutrophil infiltration around blood vessels.[15] However, histology provides only a snapshot of the inflammatory process. Because there is no functional assessment of the inflammatory cells, it cannot distinguish between inflammation due to bacterial infections and sterile inflammation due to other causes. Thus, a novel tool is needed to better our disease understanding and facilitate the development of objective diagnostics for human SSTIs.

Animal skin models are often used in the fields of cosmetics, pharmaceutics, and immunology. They are convenient models when studying skin reaction to external chemicals and other stimuli. However, animal skin models have a different structure compared to human skin, and immunologic responses are often different in animals compared to humans.[16–18]. These differences limit the ability to translate research findings from animal skin models to human disease.[19–24] Thus, the development of human skin models has been the focus of research since the early 1980s.[25] Recently, human models with complex functionality have emerged through the combination of microfluidics and tissue engineering.[26]

In the last decade, skin on a chip (SOC) has been developed to test skin responses to chemicals,[27] drugs,[28] and UV irradiation.[29] *In vitro* SOCs have been developed containing either multiple layers of cell cultures[28, 29] or 3D skin equivalents[27, 30, 31]. Various attempts have been made to closely mimic the components of skin, including resident dendritic cells,[29] vascular channels,[30] and non-contracting fibrin-based dermal matrices.[31] However, current *in vitro* SOCs is still not fully capturing cellular and structural characteristics of human skin. Also, *in vitro* SOCs require a complicated fabrication process and a long culture time from three[28] to seven days.[27] In contrast, *ex vivo* SOCs are generated by integrating *ex vivo* human skin samples into devices with[32, 33] or without other tissue components.[34] *Ex vivo* skin is obtained by a traditional 4–5 mm punch biopsy, and does not require a long incubation time unlike the *in vitro* models. Moreover, *ex vivo* SOCs provides a more accurate model. However, there are still ethical and clinical issues, namely that 4–5 mm punch biopsy leave behind a scar, and the sampling process causes the pain to the donor. In addition, *ex vivo* SOCs have a limitation in the real-time imaging due to the large sample size, requiring immunohistochemical staining.

Here, we developed an assay that enables the study of neutrophil responses to bacterial infections in a full-thickness, human microscopic skin tissue column (MSTC). We employed human skin samples collected by micro-biopsy, a minimally invasive technique that allows

healing without scarring and minimizes pain during the sampling process.[35] We integrated the harvested MSTCs into the microfluidic device and used a drop of whole blood as the source of neutrophils without an isolation process. We found that the number of migrating neutrophils correlates with the concentration of bacteria on the skin column. This suggests the motility of neutrophils as a potential biomarker for the diagnosis of SSTIs. We also used the platform to test the efficiency of antibiotic treatment, which may enable clinically relevant applications, such as antibiotic screening for treating SSTIs.

Methods

Microfluidic device fabrication:

Microfluidic channels were fabricated by soft lithography as previously reported.[36] SU-8 (Microchem) master was fabricated by standard photolithography procedure. Polydimethylsiloxane (PDMS, Sylgard 184, Corning) was mixed in a 10:1 ratio, poured onto this SU-8 master, degassed, and cured overnight. Cured PDMS was cut, and punches were used to make an inlet/outlet: 1 mm for the column loading channel (CLC), and 1.5 mm for the blood loading channel (BLC). Punched PDMS channel was bonded to 1.5 glass-bottom well plates using plasma treatment and baked at 65 °C for 30 minutes. Devices were primed with Iscove's Modified Dulbecco's Medium (IMDM) containing 10% fetal bovine serum (FBS) before use. Devices were placed under vacuum for at least 10 minutes, and IMDM with 10 % FBS was injected into the outlet of the CLC and inlet of the BLC. IMDM with 10% FBS was further added to the well until the device was completely submerged. The migration channel was allowed to be completely primed for at least 15 minutes before further use.

Harvest of full-thickness human microscopic skin tissue column (MSTC):

Multiple edged micro-biopsy needles were fabricated by honing standard 23G hypodermic needles (Exel).[37] After fabrication, the needles were sterilized in an autoclave. A sterile multi-edged needle was attached to 1 ml syringe filled with sterile silane water (0.9 %). Skin samples were obtained in sterile conditions from healthy humans undergoing elective abdominoplasty at Massachusetts General Hospital (MGH). All experiments were performed in accordance with the Declaration of Helsinki, and approved by the institutional review board (IRB) committee at MGH. Skin donors were informed regarding the possibility of excess samples being used in research and consent was obtained. The skin samples are placed on top of 12 well plates. The skin surface was wiped with a 70 % isopropanol solution and allowed to air dry completely. Multiple edged needles were inserted through the skin and withdrawn to extract the microscopic skin tissue column (MSTC). Each MSTC was transferred in 1 ml sterile saline water (0.9 %) by pushing the plunger of the syringe. Fresh skin was used to harvest MSTCs on the same day of abdominoplasty. Frozen skin was kept in saline water at −20 °C and thawed in the warm water bath at the day of the experiment.

Bacteria culture:

The SH1000-GFP *Staphylococcus aureus* strain, which is resistant to tetracycline and expresses a green fluorescent protein (GFP), was given by the laboratory of Mary Mullins at the University of Sheffield (Sheffield, UK) as a generous gift. *S. aureus* was cultured in brain

heart infusion (BHI) agar plate with 5 μg/ml tetracycline (Teknova, B1015). Single or two colonies were transferred into 10 ml of BHI broth containing 5 μg/ml tetracycline. After overnight incubation in aerobic conditions with shaking at 37 °C, 0.1 ml of bacterial suspension was added to 20 ml of BHI broth containing 5 μg/ml tetracycline and sub-cultured for 4 hours. The bacterial suspension was purified with 10 ml of pure BHI twice by centrifuge to remove tetracycline from the solution. After the purification, its concentration was adjusted based on the optical density at 600 nm.

MSTC preparation:

In this work, all MSTCs were kept completely soaked in the solution and were transferred with a solution less than 200 μl using 1 ml pipette. The solution was gently mixed using a 1 ml pipette after the transfer of columns. Besides imaging, the whole procedure is done at room temperature. Harvested human MSTCs were transferred into 7 ml of bacterial suspensions of various bacterial concentrations and incubated for 10 minutes. Control MSTCs were incubated in BHI without bacteria. After incubation, MSTCs were transferred into 7 ml BHI solution to wash redundant bacteria in solution. This washing step was repeated four times.

For antibiotic testing, one additional drug treatment step was added to the MSTC preparation. After bacteria-inoculation, the MSTCs were washed with 7 ml of BHI solution three times. The MSTCs were then transferred into 2 ml of 0.1 mg/ml Penicillin in BHI and incubated for 90 minutes. Non-treated MSTCs were incubated in 2 ml of BHI without antibiotic in this step. After the drug treatment, the MSTCs were washed four times with 7 ml of BHI solution.

SOC loading and time-lapse imaging:

After the washing steps, MSTCs were transferred into 7 ml IMDM containing 10 % FBS. Then, each MSTC was transferred into separate 1 ml IMDM containing 10 % FBS before loading into the microfluidic device. MSTCs were transferred near the inlet of the CLC, and the media was sucked from the outlet of the CLC using a pipette, transporting the MSTC into the CLC by fluid flow. IMDM with 10 % FBS in the well plate was removed. 100 μl of IMDM with 10 % FBS was then flowed through the BLC twice to remove the cytokine, potentially diffused from skin columns. 2 ml of IMDM with 10 % FBS was added into well until the device was submerged. Blood was obtained from excess, human blood samples from healthy donors, and collected in 10 ml heparin-coated vacuum tubes (Vacutainer, Becton Dickinson) at the blood donor center, MGH. Blood donors were informed regarding the possibility of excess samples being used in research and consent was obtained. Blood samples were gently mixed using a rotator until the staining step on the same day of collection. Blood was diluted with IMDM containing 10% FBS at a 1:1 ratio and stained with Hoechst 33342 at 33 μM for at least 15 minutes before loading into the device. 0.75 μl of stained, diluted human blood was then loaded into the inlet of the BLC. Devices were placed on the stage of fully automated, fluorescent Zeiss microscope heated to 37 °C with 5 % CO_2 and imaged every 10 minutes for 4 hours. Between the start of observation and blood loading, it took about 10–20 minutes to complete the set-up. The start of the

observation was considered as time zero in this study. Devices were imaged every 5 minutes when monitoring the neutrophil migration through the RBC filter.

Pre-incubation methods:

After MSTCs were loaded into SOC, the device was completely submerged in 2 ml of IMDM with 10 % FBS. Whole devices were incubated on the stage of the microscope at 37 °C with 5 % CO_2 for 4 hours. After the incubation step, devices were taken from the stage, and diluted whole blood was loaded into the inlet of the BLC. Devices were re-loaded on the stage of the microscope and monitored every 10 minutes for 4 hours while heated to 37 °C with 5 % CO_2. Since MSTCs were soaked in the bacterial suspension at extremely low concentrations, some MSTCs had no *S. aureus* even after the inoculation process. For the study, such MSTCs were excluded from the infected conditions (Fig. S4).

Data analysis:

Neutrophil counting and integration of green fluorescent intensity were processed using an ImageJ (Detail is shown in Fig. S5). Null and alternative hypotheses for the statistical analysis in Fig. 5, 6 are shown in Table S1.

Results and Discussion

Microfluidic device design:

We designed a microfluidic device to study the neutrophil migratory behavior in the context of bacterial infection. The device has three major compartments: a column loading channel (CLC), a blood loading channel (BLC), and a migration region (MR, Fig. 1b). MSTCs are harvested using a laboratory-fabricated micro-biopsy needle (Fig. 1a). The MSTCs are transferred on top of the device, close to the inlet of the CLC. Then, a negative pressure is generated by extracting the fluid at the outlet of the CLC using a pipette. As a result, MSTCs are guided into the CLC via fluid flow through the channel. The MSTC is trapped by two posts at the end of the CLC that prevent its escape through the outlet. We do not consider the orientation of columns as a critical factor of this study. This is because the total amount of chemoattract produced in the CLC does not depend on the orientation of columns. Thus, MSTCs are loaded into the channel in random orientation (Fig. 3).

One of the important features of our device is that the neutrophils are studied directly from whole blood. A neutrophil isolation step is not required. Following MSTC loading, 0.75 μl of diluted whole blood is loaded into the BLC (Fig. 1a). Because leukocytes and red blood cells (RBCs) are heavier than the serum and media, they quickly sediment to the bottom of the BLC.[38] Settling blood cells push each other and distribute uniformly over the surface of the BLC. At the edges of the BLC, blood cells also push each other towards the MR. MR consists of 39 RBC filters and 40 migration channels (MCs) (Fig. 1b). RBC filters have 4.5 × 4.2 μm cross-section. The small cross-section of the channels mechanically impedes the passive movement of RBC into the MR.[36, 38] However, the cross-section is large enough for neutrophils to squeeze themselves and autonomously pass through the filter (Fig. 1c). This small geometry also filters other leukocytes, which are larger and less deformable than neutrophils, with high specificity (> 96 %).[36] To support this point, we show that when

isolated T cells are loaded into the BLC, none of them passes through the RBC filter to migrate towards bacteria growing in the CLC (Video S1).

Column harvesting:

We harvest and load cylindrical MSTCs into the microfluidic channel. Human skin is obtained from healthy human volunteers by elective abdominoplasty. The diameter of MSTCs is controlled by the size of the biopsy needle and is 23G (internal diameter ~340 μm), comparable to the CLC width and height. The full-thickness, human MSTCs are harvested using a laboratory-fabricated micro-biopsy needle with two or three cutting edges (Fig. 2a).

We tested the effect of the number of edges on the skin column shape. When MSTCs are harvested by a two-edged needle,[35, 37] they have a significantly larger epidermis compared to the dermis (Fig. 2c). Moreover, these MSTCs have a high deviation in dermis size. Sometimes, the dermis is torn off during the harvesting process, dividing the column into two pieces. With three-edged needles, MSTCs have a more uniform, cylindrical shape (Fig. 2b): the width of the epidermis is closer to the width of the dermis layer (Fig. 2d), and the dermis width is significantly more uniform (Fig. 2e). Geometries of MSTCs show no significant variation between needles (Fig. S1). Thus, for the rest of the study, three-edged 23G needles are used to harvest the optimized columns. Previous studies have demonstrated that MTSC donor sites harvested by micro-biopsy heal without scarring, unlike the traditional punch biopsy.[35] This feature makes the technique attractive for direct harvesting of MSTCs from patients.

Monitoring the immune response to the bacterial infection:

The design of the microfluidic channels of the MR allows precise measurements of neutrophil migration from the blood sample to the skin column. Using this platform, we compared the neutrophils migratory behavior towards MSTCs with or without bacteria, as models of infected or healthy skin, respectively. In this demonstration, we harvested MSTCs from frozen/thawed skin samples.

We simulated bacterial infections by soaking MSTCs in a suspension of *S. aureus* (Fig. 1a). The number of bacteria on the columns is roughly controlled by using the bacterial suspension with various optical density (OD_{600}). The distribution of bacteria is primarily limited to the surface of the column. Although this is different from clinical cases of SSTIs, we found that it replicates key aspects of a skin infection, including the stimulation of neutrophil migration (Fig. S6).

Once MSTCs and whole blood are loaded into the SOCs, neutrophils migrate through MC. We obtained blood and skin samples from different donors. We use the same blood samples for both the control and the infected experimental situations. Further, skin columns are harvested from the same skin sample for both control and infected experiments. Compared to the control, more neutrophils migrate towards the infected MSTCs, resulting in a higher accumulation in the CLC (Fig. 3). Because neutrophils from the same donors and skin samples from the same donors are used for the control and infected conditions, the effect of the bacterial load is isolated and quantified with precision. We quantify the infection by

integrating the fluorescent intensity at 470 nm in the CLC over time. This value represents the total number of *S. aureus*, which expresses the green fluorescent protein (Fig. 4a). We quantify the migratory behavior of neutrophils by counting the total number of neutrophils reaching the CLC over time (Fig. 4b). In these quantifications, the auto-fluorescence of MSTCs is accounted for by subtracting the fluorescence intensity of an early image from the time-lapse stack (Fig. S5). The number of migrated neutrophils is plotted as a function of integrated green fluorescent intensity (Fig. 4c). The number of migrated neutrophils increases as the amount of *S. aureus* on the column increases, and scattered plots (Fig. 4a, b) collapse into one (Fig. 4d). We found distinct trends for each donor, suggesting that each blood donor shows slightly different immune responses to *S. aureus* (Fig. 4d, e). A larger number of neutrophils migrate in response to a larger bacterial load for all donors, even though the number of neutrophils migrating varies significantly between donors.

Due to the donor dependency of neutrophils migratory behavior, it is not possible to define the limit of detection for the system. Distinctive neutrophil migratory behavior represents an interesting finding from the present study. For future clinical applications, donor variability would need to be taken into account. For example, one could measure the change in neutrophil migration before and after treatment (e.g., antibiotics) or compare the neutrophil responses between an infected and uninfected skin samples. For scientific applications, animal neutrophils from the same donor could be used to obtain consistent and predictable migratory behavior.

Signal amplification for the diagnosis of SSTIs:

Neutrophils migratory behavior positively correlates with the degree of infection. This suggests that neutrophil migration in our assay may be employed as a potential biomarker for SSTIs. The bacteria concentrations in skin samples from patients with cellulitis, the most common skin infection,[2] ranges between 1×10^2 - 2×10^6 CFU/g of skin tissue.[14, 39] For MSTCs samples of 1×10^{-4} cm^3, as used in this study, a bacteria density in the range of 0 – 200 CFU/column would be expected. Thus, we tested the limit of bacteria detection on our platform.

Unfortunately, the adjustment of bacteria concentration based on optical density provides only rough control over the bacterial load on the column. As a previous study shows, even when tissue samples are soaked in the same bacterial suspension, significantly different bacterial loads may result, sometimes different by more than an order of magnitude[40]. Therefore, it is not possible to use one column for CFU counting and another for the skin on a chip assay. Given our results demonstrate neutrophil migration is proportional to bacterial load (Fig. 4), it is necessary to simultaneously estimate the bacteria number on each skin column while monitoring the neutrophil migration. Thus, we estimate the initial amount of bacteria on the column by converting the fluorescent intensity to colony-forming units (CFU). We measure the integrated fluorescent intensity at 4 hours and compare the value of MSTCs to that of a single colony inside the device (Fig. S2a, b). After 4 hour-incubation, we measure a fluorescence intensity of 0.852 ± 0.400 (arbitrary units, N = 21) for 1 CFU (Fig. S2c). We verify that integrated intensity is linearly proportional to CFU (Fig. S3a). The integrated fluorescent intensity in the CLC is divided by that of one CFU to quantify the

initial bacterial load on the column. Fig. 3 and 4 show the range of bacteria concentration of 3×10^2 - 1×10^4 CFU/column, corresponding to 3×10^6 - 1×10^8 CFU/g.

To accomplish the detection at clinically relevant bacteria densities, we amplify the infection signal by pre-incubating the MSTCs before blood loading (Fig. 5). In this demonstration, MSTCs are harvested from frozen/thawed skin samples. We loaded MSTCs with clinically relevant bacteria concentration. In two independent trials, infected MSTCs show 9.9 ± 12.9 and 5.5 ± 5.0 fluorescent intensity/column after 4 hour-incubation, respectively. These values are corresponding to 11.7 ± 19.7 and 6.5 ± 5.9 CFU/column (~ $1.2 \times 10^5 \pm 2.0 \times 10^5$ and $6.5 \times 10^4 \pm 5.9 \times 10^4$ CFU/g). Half of the devices with infected MSTCs are tested without amplification (Fig. 5a), and another half are incubated in SOCs at 37 °C for 4 hours before blood loading (Fig. 5b, c). Amplified, infected condition (*I4*) shows a significantly higher neutrophil migration than its control (*C4*) at 4 hours after blood loading while non-amplified ones (*I* and *C*) do not (Fig. 5d).

Our platform and pre-incubation procedure enable more rapid measurements compared to traditional CFU counting on the plate. Whereas the traditional culture methods require more than 24 hours,[14, 39] our method provides results in eight hours. Moreover, our approach does not require tissue homogenization, which causes damage to pathogen and skin tissue, potentially providing more accurate measurements.

Antibiotic testing:

Ex vivo SOC can be utilized to evaluate the efficiency of antibiotic treatment by monitoring the change in the immune response. Such evaluations may help test and compare various treatments on human tissue samples before applying the same treatment to the patients. This concept could eventually bring personalized antibiotic testing to emergency rooms and primary care offices.

As proof of principle demonstration, we tested the effect of penicillin treatment on the *S. aureus* inoculated MSTCs. In this demonstration, we harvest *ex vivo* MSTCs from fresh skin samples. Harvested MSTCs are soaked in bacterial suspension and penicillin solution depending on the conditions. There are four conditions in this study: control without (*C*) and with penicillin treatment (*CP*), and the infected condition without (*I*) and with penicillin treatment (*IP*). MTSCs are washed to remove the penicillin in the solution before loading into the device. *C* and *CP* show no significant difference in the neutrophil migration indicating that penicillin in the solution is either efficiently removed during the washing steps or does not affect the neutrophil migration (Fig. 6e, h).

Only the infected, untreated samples *(I)* show clear bacteria growth over time (Fig. 6a–c, f). Infected samples (*I*) also show higher initial neutrophil accumulation near the column compared to *IP* (Fig. 6a, b, d, g). The number of migrated neutrophils at 4 hours is also significantly higher (red stars, Fig. 6e, h). The results suggest that penicillin treatment reduces the bacterial growth on the MSTCs and attenuates neutrophils migration. *C*, *CP*, and *IP* show no significant difference in the neutrophil migration (Fig. 6e). Interestingly, when larger amounts of *S. aureus* are inoculated (Fig. 6c, f), *IP* samples show significantly higher neutrophil migration compared to *C* and *CP* (Fig. 6h). The results suggest that higher

infection loads may require larger amounts of antibiotic. Testing various antibiotics at various doses using *ex vivo* SOC could provide a practical way to estimate the optimal antibiotic and dose for each patient. SOC may also augment the physician's ability to differentiate cellulitis from pseudo-cellulitis, a group of non-infectious skin etiologies that mimic the signs and symptoms of cellulitis without the microbes[4, 41]. If the application of antibiotics to a patient skin sample does not change the migration of neutrophils, a diagnostic of pseudo-cellulitis could be more likely.

Conclusion

In this study, we combine microfluidics with a micro-biopsy technique to make a novel, microscopic, human *ex vivo* SOC. The extent of neutrophil migration correlates with the number of bacteria on the MSTC, suggesting neutrophils as a potential diagnostic biomarker for SSTIs. By pre-incubating MSTCs, our platform detects bacterial concentrations within a clinically meaningful range while ensuring a quick measurement. We also demonstrate that our assay can measure the efficiency of antibiotic treatment. The micro-biopsy technique can directly collect the skin tissue sample from a patient, making our platform appealing for diagnosis. This article shows a proof-of-principle for utilizing microscopic, human *ex vivo* SOC for diagnosis. More studies would be required to gain an in-depth understanding of the mechanism of neutrophil migration and donor dependency. Future studies will also test the ability of the assay to distinguish between cellulitis and pseudo-cellulitis patient samples. We envision that this platform will expand the current understanding of SSTIs and form the basis for innovative diagnostic strategies.

Supplementary Material

Refer to Web version on PubMed Central for supplementary material.

Acknowledgment

This work is funded in part by grants from the Wellman Center Early Discovery Fund (MedCap) and form the National Institute of Health (awards EB002503 and GM092804). We thank our colleagues at the BioMEMS Resource Center, Massachusetts General Hospital, and in particular, Dr. Xiao Wang for the insightful discussion and Mr. Octavio Hurtado for the help with device fabrication.

References

1. Hersh AL, Chambers HF, Maselli JH and Gonzales R, Archives of internal medicine, 2008, 168, 1585–1591. [PubMed: 18663172]
2. Miller LG, Eisenberg DF, Liu H, Chang CL, Wang Y, Luthra R, Wallace A, Fang C, Singer J and Suaya JA, BMC infectious diseases, 2015, 15, 362. [PubMed: 26293161]
3. Handbook D, Baltimore: HCIA, Ernst & Young LLP, 2000.
4. Weng QY, Raff AB, Cohen JM, Gunasekera N, Okhovat JP, Vedak P, Joyce C, Kroshinsky D and Mostaghimi A, JAMA dermatology, 2017, 153, 141–146. [PubMed: 27806170]
5. Levell N, Wingfield C and Garioch J, British journal of dermatology, 2011, 164, 1326–1328. [PubMed: 21564054]
6. David CV, Chira S, Eells SJ, Ladrigan M, Papier A, Miller LG and Craft N, Dermatology online journal, 2011, 17, 1.
7. Arakaki RY, Strazzula L, Woo E and Kroshinsky D, JAMA dermatology, 2014, 150, 1056–1061. [PubMed: 25143179]

8. Krasagakis K, Valachis A, Maniatakis P, Krüger-Krasagakis S, Samonis G and Tosca AD, International journal of dermatology, 2010, 49, 1012–1017. [PubMed: 20931671]
9. Lazzarini L, Conti E, Tositti G and de Lalla F, The Journal of infection, 2005, 51, 383–389. [PubMed: 16321649]
10. Hook EW 3rd, Hooton TM, Horton CA, Coyle MB, Ramsey PG and Turck M, Archives of internal medicine, 1986, 146, 295–297. [PubMed: 3947189]
11. Pallin DJ, Bry L, Dwyer RC, Lipworth AD, Leung DY, Camargo CA Jr., Kupper TS, Filbin MR and Murphy GF, PloS one, 2016, 11, e0162947. [PubMed: 27656884]
12. Chira S and Miller L, Epidemiology & Infection, 2010, 138, 313–317. [PubMed: 19646308]
13. Gunderson CG and Martinello RA, The Journal of infection, 2012, 64, 148–155. [PubMed: 22101078]
14. Duvanel T, Auckenthaler R, Rohner P, Harms M and Saurat JH, Archives of internal medicine, 1989, 149, 293–296. [PubMed: 2644902]
15. McKee PH, Calonje E, Lazar A and Brenn T, McKee's Pathology of the Skin: With Clinical Correlations, Elsevier Saunders, 2012.
16. Serpell J, In the company of animals: A study of human-animal relationships, Cambridge University Press, 1996.
17. Watson ME Jr., Neely MN and Caparon MG, in Streptococcus pyogenes : Basic Biology to Clinical Manifestations, eds. Ferretti JJ, Stevens DLand Fischetti VA, Oklahoma City (OK), 2016.
18. Schmook FP, Meingassner JG and Billich A, International journal of pharmaceutics, 2001, 215, 51–56. [PubMed: 11250091]
19. Seok J, Warren HS, Cuenca AG, Mindrinos MN, Baker HV, Xu W, Richards DR, McDonald-Smith GP, Gao H, Hennessy L, Finnerty CC, Lopez CM, Honari S, Moore EE, Minei JP, Cuschieri J, Bankey PE, Johnson JL, Sperry J, Nathens AB, Billiar TR, West MA, Jeschke MG, Klein MB, Gamelli RL, Gibran NS, Brownstein BH, Miller-Graziano C, Calvano SE, Mason PH, Cobb JP, Rahme LG, Lowry SF, Maier RV, Moldawer LL, Herndon DN, Davis RW, Xiao W, Tompkins RG, Inflammation and L. S. C. R. P. Host Response to Injury, Proceedings of the National Academy of Sciences of the United States of America, 2013, 110, 3507–3512. [PubMed: 23401516]
20. Warren HS, Fitting C, Hoff E, Adib-Conquy M, Beasley-Topliffe L, Tesini B, Liang X, Valentine C, Hellman J, Hayden D and Cavaillon JM, The Journal of infectious diseases, 2010, 201, 223–232. [PubMed: 20001600]
21. Mestas J and Hughes CC, The Journal of Immunology, 2004, 172, 2731–2738. [PubMed: 14978070]
22. Fowler VG Jr and Proctor RA, Clinical Microbiology and Infection, 2014, 20, 66–75. [PubMed: 24476315]
23. Pound P and Bracken MB, Bmj, 2014, 348, g3387. [PubMed: 24879816]
24. Kola I and Landis J, Nature reviews Drug discovery, 2004, 3, 711. [PubMed: 15286737]
25. Bell E, Ehrlich HP, Buttle DJ and Nakatsuji T, Science, 1981, 211, 1052–1054. [PubMed: 7008197]
26. Bhatia SN and Ingber DE, Nature biotechnology, 2014, 32, 760–772.
27. Abaci HE, Gledhill K, Guo Z, Christiano AM and Shuler ML, Lab on a chip, 2015, 15, 882–888. [PubMed: 25490891]
28. Wufuer M, Lee G, Hur W, Jeon B, Kim BJ, Choi TH and Lee S, Scientific reports, 2016, 6, 37471. [PubMed: 27869150]
29. Ramadan Q and Ting FC, Lab on a chip, 2016, 16, 1899–1908. [PubMed: 27098052]
30. Mori N, Morimoto Y and Takeuchi S, Biomaterials, 2017, 116, 48–56. [PubMed: 27914266]
31. Sriram G, Alberti M, Dancik Y, Wu B, Wu R, Feng Z, Ramasamy S, Bigliardi PL, Bigliardi-Qi M and Wang Z, Materials Today, 2018, 21, 326–340.
32. Wagner I, Materne EM, Brincker S, Sussbier U, Fradrich C, Busek M, Sonntag F, Sakharov DA, Trushkin EV, Tonevitsky AG, Lauster R and Marx U, Lab on a chip, 2013, 13, 3538–3547. [PubMed: 23648632]

33. Maschmeyer I, Lorenz AK, Schimek K, Hasenberg T, Ramme AP, Hubner J, Lindner M, Drewell C, Bauer S, Thomas A, Sambo NS, Sonntag F, Lauster R and Marx U, Lab on a chip, 2015, 15, 2688–2699. [PubMed: 25996126]

34. Atac B, Wagner I, Horland R, Lauster R, Marx U, Tonevitsky AG, Azar RP and Lindner G, Lab on a chip, 2013, 13, 3555–3561. [PubMed: 23674126]

35. Tam J, Wang Y, Farinelli WA, Jiménez-Lozano J, Franco W, Sakamoto FH, Cheung EJ, Purschke M, Doukas AG and Anderson RR, Plastic and Reconstructive Surgery Global Open, 2013, 1.

36. Ellett F, Jorgensen J, Marand AL, Liu YM, Martinez MM, Sein V, Butler KL, Lee J and Irimia D, Nat Biomed Eng, 2018, 2, 207–214. [PubMed: 30283724]

37. Tam J, Farinelli W, Franco W and Anderson RR, Journal of visualized experiments : JoVE, 2018, DOI: 10.3791/58289.

38. Hamza B and Irimia D, Lab on a chip, 2015, 15, 2625–2633. [PubMed: 25987163]

39. Crisp JG, Takhar SS, Moran GJ, Krishnadasan A, Dowd SE, Finegold SM, Summanen PH, Talan DA and E. M. I. N. S. Group, Clinical infectious diseases : an official publication of the Infectious Diseases Society of America, 2015, 61, 1679–1687. [PubMed: 26240200]

40. Veloso TR, Claes J, Van Kerckhoven S, Ditkowski B, Hurtado-Aguilar LG, Jockenhoevel S, Mela P, Jashari R, Gewillig M, Hoylaerts MF, Meyns B and Heying R, The Journal of thoracic and cardiovascular surgery, 2018, 155, 325–332 e324. [PubMed: 28712577]

41. Raff AB and Kroshinsky D, Jama, 2016, 316, 325–337. [PubMed: 27434444]

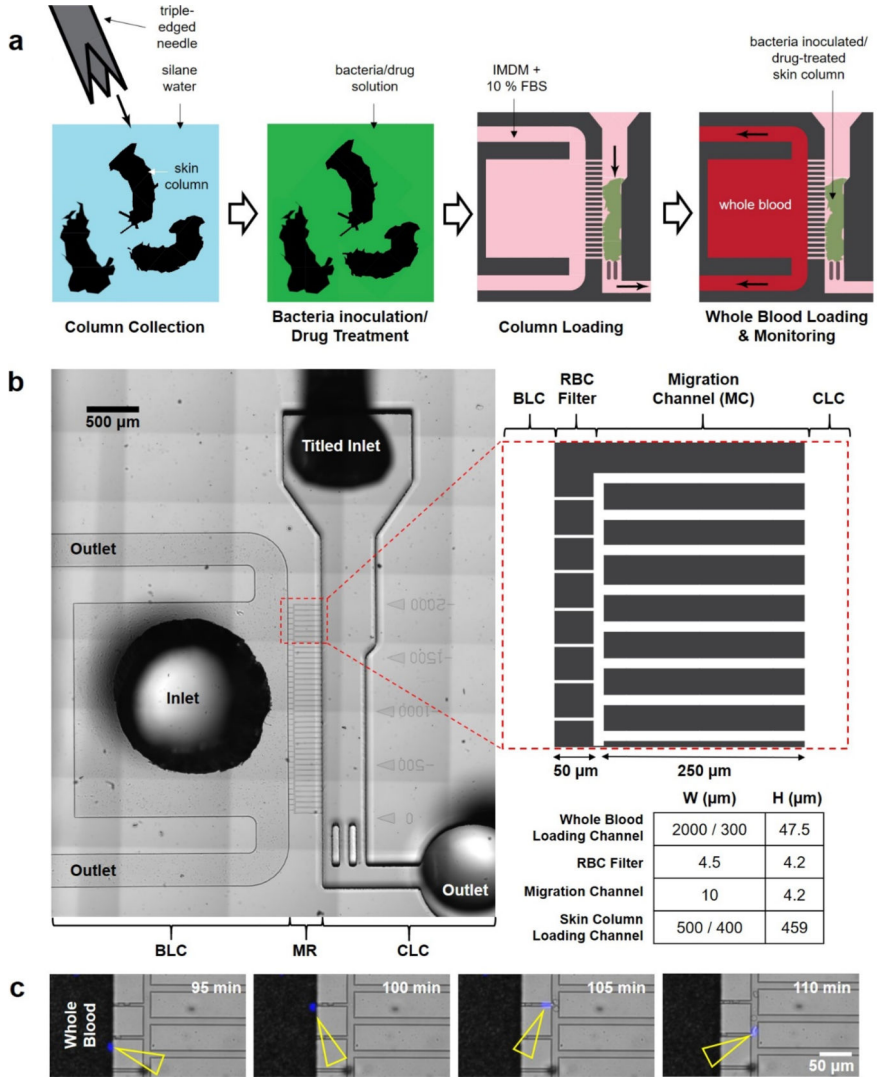

Fig. 1.

Ex vivo SOC assay for the diagnosis of SSTIs. (a) Schematics of the human skin and blood samples loading. (b) Microfluidic design of e*x vivo* SOC. Left shows the bright field image of *ex vivo* SOC. Top-right represents the design of the migration channel. Bottom-right shows the dimension of *ex vivo* SOC components: whole blood loading channel (BLC), RBC filter, migration channel (MC), and skin column loading channel (CLC). (c) Time-lapse images show the neutrophil migration through the RBC filter while RBCs are blocked.

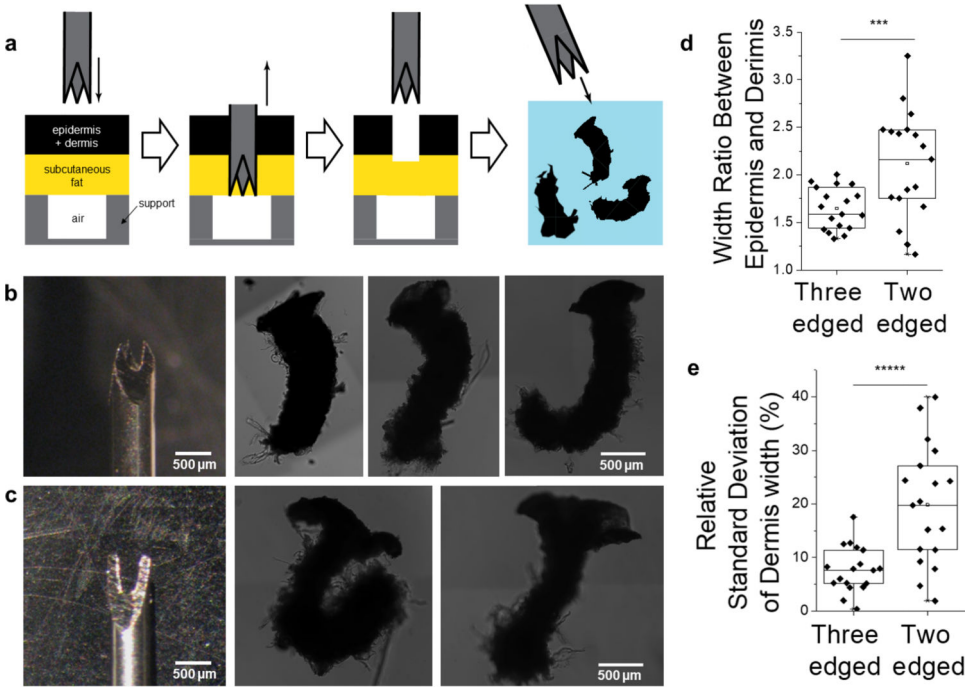

Fig. 2.

Harvesting of full-thickness human MSTCs using micro biopsy techniques. (a) Schematics of MSTC harvesting using skin samples. (b) Image of a triple-edged micro-biopsy needle and harvested MSTCs. (c) Image of a double-edged micro-biopsy needle and harvested MSTCs. (d) The relative width between epidermis and dermis of MSTCs. n = 18 samples, n = 3 needles. (e) The relative standard deviation of the dermis width of MSTCs. For the quantification, the width of the dermis is measured at three points from the top, middle, and bottom of each MSTCs. Brightness and contrast are adjusted to clearly show the edge of MSTCs. n = 3 needles, n = 6 MSTCs per needle. **** $p \leq 0.005$, ***** $p \leq 0.0005$.

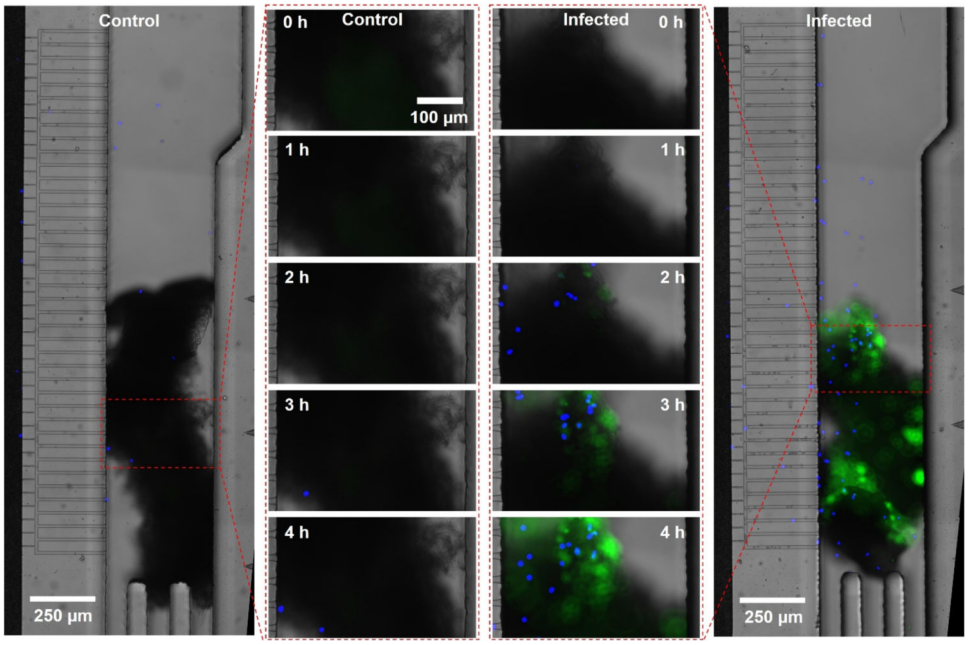

Fig. 3.

Neutrophil migration toward full-thickness human MTSC. Representative images showing neutrophil migration in SOC with the control (left) and bacteria-inoculated MTSC (right). Blue and green represent the Hoechst stained nucleus of neutrophils and GFP-expressing *S. aureus*, respectively. The left and right images show the images at t = 4 h. Time-lapse images of the red boxed area are shown in the middle. Auto-fluorescence in the DAPI channel of MSTCs is removed in this figure by subtracting the image at the early stage from the time-lapse. Brightness and contrast are adjusted to clearly show neutrophils and *S. aureus*.

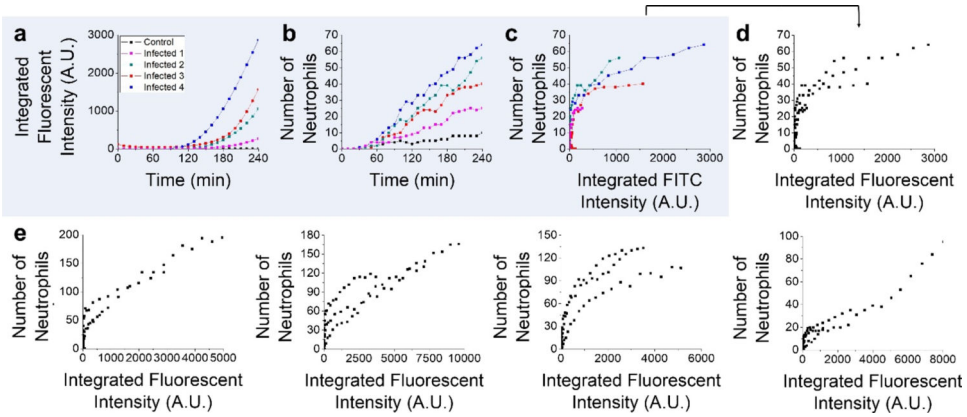

Fig. 4.

The number of migrated neutrophils for various MSTC infection loads. (a) Integrated green fluorescent intensity of the CLC over time. (b) The number of neutrophils in the CLC over time. (c) The number of migrated neutrophils as a function of integrated green fluorescent intensity. Data points collected from the same MSTC are marked in the same color through a-c. (d) The correlation between the number of migrated neutrophils and the degree of infection of MSTC, the total amount of bacteria. (e) Data points obtained from each blood donor. Each plot in Fig. 4d and e shows the data obtained with five distinct blood donors. Each donor shows a distinct trend. Besides the last plot of Fig. 4e, all plots were obtained with MSTCs harvested from the same skin sample. Each dot represents the result analyzed at each time point. n = 5 experiments, n = 4 or 5 MSTCs per experiment, n = 25 time points per MSTC.

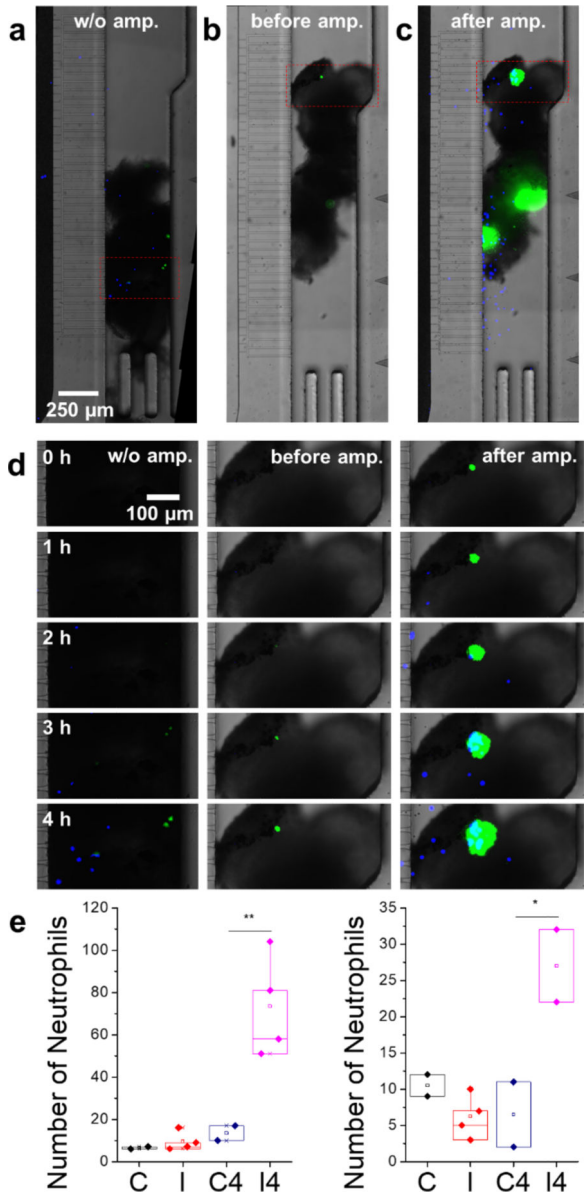

Fig. 5.

Pre-incubation for detecting a small number of bacteria on MSTCs. (a-c) Representative images are showing bacteria-inoculated MSTCs in SOC without amplification (a), before amplification (b), and after amplification (c). a and c is taken 4 hours after blood loading. b is taken after 4-hour incubation and right before the blood loading. (d) Time-lapse images of the red boxed area (a-c). (e) Number of migrated neutrophils 4-hour after blood loading. Each plot shows the result of the independent experiment. Amplified, infected condition (*I4*) show a significantly higher signal than its control (*C4*) while there is no significant difference between non-amplified cases (*C* and *I*). Each dot represents the data from each MSTCs at 4 hours. Auto-fluorescence in the DAPI channel of MSTCs is removed in this figure by subtracting the image at the early stage from the time-lapse. Brightness and

contrast are adjusted to clearly show neutrophils and *S. aureus*. n = 2 experiments, n = 10 or 12 MSTCs per experiment. * $P \leq 0.05$, ** $P \leq 0.01$.

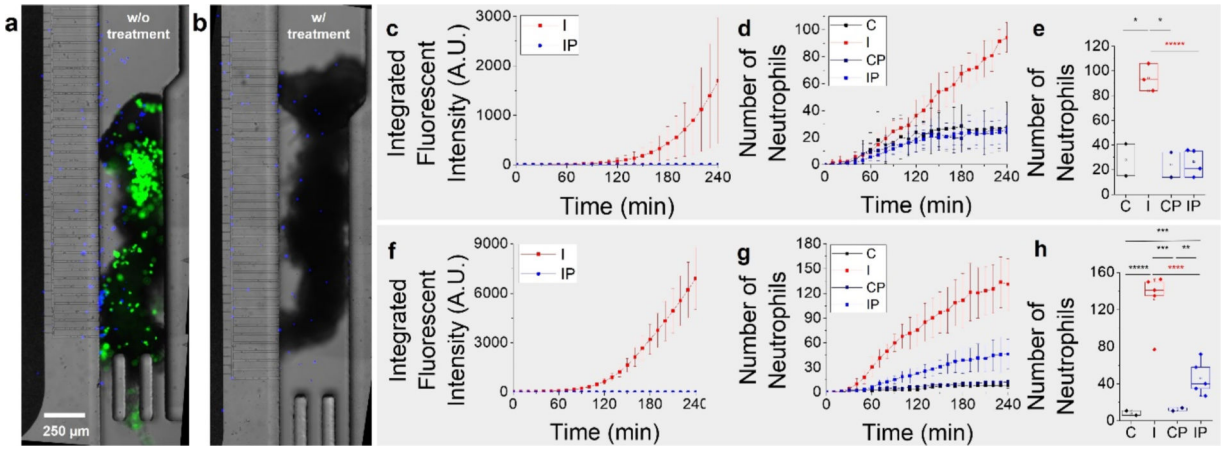

Fig. 6.

Antibiotic tests using *ex vivo* SOC. (a, b) Representative images are showing infected MSTCs in *ex vivo* SOC without (a) / with (b) penicillin treatment. Fig. 6a and b are taken 4 hours after blood loading. (c-h) Rows c-e and f-h show the results of two independent experiments, comparing control (C) and infected (I) skin samples, with and without Penicillin (P) treatment. (c, f) Integrated green fluorescent intensity over time. (d, g) The number of migrated neutrophils over time. Error bar represents the standard deviation. (e, h) The number of migrated neutrophils at 4 hours. Penicillin treatment reduces the degree of a skin infection, resulting in a significantly lower neutrophil migration (red stars shown in e, h). Auto-fluorescence in the DAPI channel of MSTCs is removed in this figure by subtracting the image at the early stage from the time-lapse. Brightness and contrast are adjusted to clearly show neutrophils and *S. aureus*. n = 2 experiments, n = 11 or 14 MSTCs per experiment. * $P \leq 0.05$, ** $P \leq 0.01$, *** $P \leq 0.005$, **** $P \leq 0.001$, ***** $P \leq 0.0005$